CERN-PPE/90-195
20 December 1990

EUROPEAN ORGANIZATION FOR NUCLEAR RESEARCH

Measurement of the B hadron lifetime

The ALEPH Collaboration*

Abstract

The average lifetime of B hadrons has been measured by the ALEPH experiment at LEP. Events containing B hadrons are selected by the identification of leptons with high transverse momentum in hadronic Z decays, and the lifetime is extracted from a fit to the impact parameter distribution of the lepton tracks. From a sample of 1.7×10^5 hadronic Z decays a lifetime of $1.29 \pm 0.06 \pm 0.10$ ps is measured.

(Submitted to Physics Letters B)

*See the following pages for the list of authors.

The ALEPH Collaboration

D. Decamp, B. Deschizeaux, C. Goy, J.-P. Lees, M.-N. Minard

Laboratoire de Physique des Particules (LAPP), IN²P³-CNRS, 74019 Annecy-le-Vieux Cedex, France

R. Alemany, J.M. Crespo, M. Delfino, E. Fernandez, V. Gaitan, Ll. Garrido, P. Mato, R. Miquel, Ll.M. Mir, S. Orteu, A. Pacheco, J.A. Perlas, E. Tubau

Laboratorio de Fisica de Altas Energias, Universidad Autonoma de Barcelona, 08193 Bellaterra (Barcelona), Spain[9]

M.G. Catanesi, D. Creanza, M. de Palma, A. Farilla, G. Iaselli, G. Maggi, M. Maggi, S. Natali, S. Nuzzo, M. Quattromini, A. Ranieri, G. Raso, F. Romano, F. Ruggieri, G. Selvaggi, L. Silvestris, P. Tempesta, G. Zito

INFN Sezione di Bari e Dipartimento di Fisica dell' Università, 70126 Bari, Italy

Y. Gao, H. Hu[22] D. Huang, X. Huang, J. Lin, J. Lou, C. Qiao[22] T. Ruan[22] Wang, Y. Xie, D. Xu, R. Xu, J. Zhang, W. Zhao

Institute of High-Energy Physics, Academia Sinica, Beijing, The People's Republic of China[10]

H. Albrecht[2] W.B. Atwood[3] F. Bird, E. Blucher, G. Bonvicini, F. Bossi, D. Brown, T.H. Burnett[4] H. Drevermann, F. Dydak, R.W. Forty, C. Grab, R. Hagelberg, S. Haywood, B. Jost, M. Kasemann, G. Kellner, J. Knobloch, A. Lacourt, I. Lehraus, T. Lohse, D. Lüke[2] A. Marchioro, M. Martinez, J. May[2] S. Menary, A. Minten, A. Miotto, J. Nash, P. Palazzi, F. Ranjard, G. Redlinger, A. Roth, J. Rothberg[4] H. Rotscheidt, W. von Rüden, R. St.Denis, D. Schlatter, M. Takashima, M. Talby[5] W. Tejessy, H. Wachsmuth, S. Wasserbaech, S. Wheeler, W. Wiedenmann, W. Witzeling, J. Wotschack

European Laboratory for Particle Physics (CERN), 1211 Geneva 23, Switzerland

Z. Ajaltouni, M. Bardadin-Otwinowska, A. Falvard, R. El Fellous, P. Gay, J. Harvey, P. Henrard, J. Jousset, B. Michel, J-C. Montret, D. Pallin, P. Perret, J. Proriol, F. Prulhière, G. Stimpfl

Laboratoire de Physique Corpusculaire, Université Blaise Pascal, IN²P³-CNRS, Clermont-Ferrand, 63177 Aubière, France

J.D. Hansen, J.R. Hansen, P.H. Hansen, R. Møllerud, E.R. Nielsen, B.S. Nilsson

Niels Bohr Institute, 2100 Copenhagen, Denmark[11]

I. Efthymiopoulos, E. Simopoulou, A. Vayaki

Nuclear Research Center Demokritos (NRCD), Athens, Greece

J. Badier, A. Blondel, G. Bonneaud, J. Bourotte, F. Braems, J.C. Brient, G. Fouque, A. Gamess, R. Guirlet, A. Rosowsky, A. Rougé, M. Rumpf, R. Tanaka, H. Videau

Laboratoire de Physique Nucléaire et des Hautes Energies, Ecole Polytechnique, IN²P³-CNRS, 91128 Palaiseau Cedex, France

D.J. Candlin, E. Veitch

Department of Physics, University of Edinburgh, Edinburgh EH9 3JZ, United Kingdom[12]

G. Parrini

Dipartimento di Fisica, Università di Firenze, INFN Sezione di Firenze, 50125 Firenze, Italy

M. Corden, C. Georgiopoulos, M. Ikeda, J. Lannutti, D. Levinthal,[17] M. Mermikides, L. Sawyer

Supercomputer Computations Research Institute and Dept. of Physics, Florida State University, Tallahassee, FL 32306, USA[14,15,16]

A. Antonelli, R. Baldini, G. Bencivenni, G. Bologna,[6] P. Campana, G. Capon, V. Chiarella, B. D'Ettorre-Piazzoli,[7] G. Felici, P. Laurelli, G. Mannocchi,[7] F. Massimo-Brancaccio, F. Murtas, G.P. Murtas, G. Nicoletti, L. Passalacqua, M. Pepe-Altarelli, P. Picchi,[6] P. Zografou

Laboratori Nazionali dell'INFN (LNF-INFN), 00044 Frascati, Italy

B. Altoon, O. Boyle, A.W. Halley, I. ten Have, J.L. Hearns, J.G. Lynch, W.T. Morton, C. Raine, J.M. Scarr, K. Smith, A.S. Thompson, R.M. Turnbull

Department of Physics and Astronomy, University of Glasgow, Glasgow G12 8QQ, United Kingdom[12]

B. Brandl, O. Braun, R. Geiges, C. Geweniger, P. Hanke, V. Hepp, E.E. Kluge, Y. Maumary, A. Putzer, B. Rensch, A. Stahl, K. Tittel, M. Wunsch

Institut für Hochenergiephysik, Universität Heidelberg, 6900 Heidelberg, Fed. Rep. of Germany[18]

A.T. Belk, R. Beuselinck, D.M. Binnie, W. Cameron, M. Cattaneo, P.J. Dornan, S. Dugeay, A.M. Greene, J.F. Hassard, N.M. Lieske, S.J. Patton, D.G. Payne, M.J. Phillips, J.K. Sedgbeer, G. Taylor, I.R. Tomalin, A.G. Wright

Department of Physics, Imperial College, London SW7 2BZ, United Kingdom[12]

P. Girtler, D. Kuhn, G. Rudolph

Institut für Experimentalphysik, Universität Innsbruck, 6020 Innsbruck, Austria[20]

C.K. Bowdery,[1] T.J. Brodbeck, A.J. Finch, F. Foster, G. Hughes, N.R. Keemer, M. Nuttall, A. Patel, B.S. Rowlingson, T. Sloan, S.W. Snow, E.P. Whelan

Department of Physics, University of Lancaster, Lancaster LA1 4YB, United Kingdom[12]

T. Barczewski, L.A.T. Bauerdick, K. Kleinknecht, B. Renk, S. Roehn, H.-G. Sander, M. Schmelling, H. Schmidt, F. Steeg

Institut für Physik, Universität Mainz, 6500 Mainz, Fed. Rep. of Germany[18]

J-P. Albanese, J-J. Aubert, C. Benchouk, V. Bernard, A. Bonissent, D. Courvoisier, F. Etienne, S. Papalexiou, P. Payre, B. Pietrzyk, Z. Qian

Centre de Physique des Particules, Faculté des Sciences de Luminy, IN^{2}P^3-CNRS, 13288 Marseille, France

W. Blum, P. Cattaneo, G. Cowan, B. Dehning, H. Dietl, M. Fernandez-Bosman, T. Hansl-Kozanecka,[23] A. Jahn, W. Kozanecki,[3,24] E. Lange, G. Lütjens, G. Lutz, W. Männer, H-G. Moser, Y. Pan, R. Richter, J. Schröder, A.S. Schwarz, R. Settles, U. Stierlin, J. Thomas, G. Wolf

Max-Planck-Institut für Physik und Astrophysik, Werner-Heisenberg-Institut für Physik, 8000 München, Fed. Rep. of Germany[18]

V. Bertin, G. de Bouard, J. Boucrot, O. Callot,[1] X. Chen, A. Cordier, M. Davier, G. Ganis, J.-F. Grivaz, Ph. Heusse, P. Janot, V. Journé, D.W. Kim,[21] J. Lefrançois, A.-M. Lutz, J.-J. Veillet, I. Videau, Z. Zhang, F. Zomer

Laboratoire de l'Accéléateur Linéaire, Université de Paris-Sud, IN^{2}P^3-CNRS, 91405 Orsay Cedex, France

S.R. Amendolia, G. Bagliesi, G. Batignani, L. Bosisio, U. Bottigli, C. Bradaschia, M. Carpinelli, M.A. Ciocci, R. Dell'Orso, I. Ferrante, F. Fidecaro, L. Foà, E. Focardi, F. Forti, A. Giassi, M.A. Giorgi, F. Ligabue, A. Lusiani, E.B. Mannelli, P.S. Marrocchesi, A. Messineo, L. Moneta, F. Palla, G. Sanguinetti, J. Steinberger, R. Tenchini, G. Tonelli, G. Triggiani, C. Vannini-Castaldi, A. Venturi, P.G. Verdini, J. Walsh

Dipartimento di Fisica dell'Università, INFN Sezione di Pisa, e Scuola Normale Superiore, 56010 Pisa, Italy

J.M. Carter, M.G. Green, P.V. March, T. Medcalf, I.S. Quazi, M.R. Saich, J.A. Strong, R.M. Thomas, L.R. West, T. Wildish

Department of Physics, Royal Holloway & Bedford New College, University of London, Surrey TW20 OEX, United Kingdom[12]

D.R. Botterill, R.W. Clifft, T.R. Edgecock, M. Edwards, S.M. Fisher, T.J. Jones, P.R. Norton, D.P. Salmon, J.C. Thompson

Particle Physics Dept., Rutherford Appleton Laboratory, Chilton, Didcot, OXON OX11 OQX, United Kingdom[12]

B. Bloch-Devaux, P. Colas, C. Klopfenstein, E. Lançon, E. Locci, S. Loucatos, E. Monnier, P. Perez, F. Perrier, J. Rander, J.-F. Renardy, A. Roussarie, J.-P. Schuller, J. Schwindling

Département de Physique des Particules Élémentaires, CEN-Saclay, 91191 Gif-sur-Yvette Cedex, France[19]

J.G. Ashman, C.N. Booth, C. Buttar, R. Carney, S. Cartwright, F. Combley, M. Dinsdale, M. Dogru, F. Hatfield, J. Martin, D. Parker, P. Reeves, L.F. Thompson

Department of Physics, University of Sheffield, Sheffield S3 7RH, United Kingdom[12]

S. Brandt, H. Burkhardt, C. Grupen, H. Meinhard, L. Mirabito, E. Neugebauer, U. Schäfer, H. Seywerd

Fachbereich Physik, Universität Siegen, 5900 Siegen, Fed. Rep. of Germany[18]

G. Apollinari, G. Giannini, B. Gobbo, F. Liello, L. Rolandi, U. Stiegler

Dipartimento di Fisica, Università di Trieste e INFN Sezione di Trieste, 34127 Trieste, Italy

L. Bellantoni, J.F. Boudreau, D. Cinabro, J.S. Conway, D.F. Cowen,[25] A.J. DeWeerd, Z. Feng, D.P.S. Ferguson, Y.S. Gao, J. Grahl, J.L. Harton, J. Hilgart, J.E. Jacobsen, R.C. Jared,[8] R.P. Johnson, B.W. LeClaire, Y.B. Pan, J.R. Pater, Y. Saadi, V. Sharma, M.A. Walsh, J.A. Wear, F.V. Weber, M.H. Whitney, Sau Lan Wu, Z.L. Zhou, G. Zobernig

Department of Physics, University of Wisconsin, Madison, WI 53706, USA[13]

---

[1] Now at CERN.
[2] Permanent address: DESY, Hamburg, Fed. Rep. of Germany.
[3] On leave of absence from SLAC, Stanford, CA 94309, USA.
[4] On leave of absence from University of Washington, Seattle, WA 98195, USA.
[5] Also Centre de Physique des Particules, Faculté des Sciences, Marseille, France
[6] Also Istituto di Fisica Generale, Università di Torino, Torino, Italy.
[7] Also Istituto di Cosmo-Geofisica del C.N.R., Torino, Italy.
[8] Permanent address: LBL, Berkeley, CA 94720, USA.
[9] Supported by CAICYT, Spain.
[10] Supported by the National Science Foundation of China.
[11] Supported by the Danish Natural Science Research Council.
[12] Supported by the UK Science and Engineering Research Council.
[13] Supported by the US Department of Energy, contract DE-AC02-76ER00881.
[14] Supported by the US Department of Energy, contract DE-FG05-87ER40319.
[15] Supported by the NSF, contract PHY-8451274.
[16] Supported by the US Department of Energy, contract DE-FC0S-85ER250000.
[17] Supported by SLOAN fellowship, contract BR 2703.
[18] Supported by the Bundesministerium für Forschung und Technologie, Fed. Rep. of Germany.
[19] Supported by the Institut de Recherche Fondamentale du C.E.A..
[20] Supported by Fonds zur Förderung der wissenschaftlichen Forschung, Austria.
[21] Supported by the Korean Science and Engineering Foundation and Ministry of Education.
[22] Supported by the World Laboratory.
[23] On leave of absence from MIT, Cambridge, MA 02139, USA.
[24] Supported by Alexander von Humboldt Fellowship, Germany.
[25] Now at California Institute of Technology, Pasadena, California, USA.

1 Introduction

The lifetime of hadrons containing the b quark is determined in the Standard Model by the strength of the coupling of the b quark to the c and u quarks. A measurement of the lifetime is therefore of interest as it constrains fundamental parameters of the Standard Model, the parameters of quark flavour mixing.

Over the past few years this measurement has been pursued by numerous experiments [1], but the experimental uncertainty remains substantial. The advent of the e^+e^- collider LEP presents the opportunity for a higher precision measurement: at the new machine, Z particles are produced in large numbers, and decay to b quarks with a substantial branching ratio ($\sim$ 22% of hadronic decays) and with lower charm background than is found in the e^+e^- continuum.

Presented here is an analysis of data taken by the ALEPH experiment at LEP, at centre-of-mass energy on and around the Z peak. The data sample consists of about 170,000 hadronic Z decays, corresponding to an integrated luminosity of 7.7 pb^{-1}, taken during the eight months that the experiment was run in 1989 and 1990. Events containing B hadrons are selected by identifying electrons and muons from the semileptonic decay of the hadron, with high transverse momentum p_T relative to an associated jet axis. The lifetime is then extracted from a maximum likelihood fit to the impact parameter distribution of the lepton tracks, measured relative to the estimated e^+e^- interaction point.

Strictly speaking the measurement is an average over the lifetimes of all the hadrons containing b quarks, weighted by their production rates and semileptonic branching ratios, and may therefore differ from other measurements at lower energies and with different selection requirements. However, the first experimental checks of the separate lifetimes of the various species [2] support the theoretical expectation that these differences are small.

A silicon microvertex detector was partially installed during the data taking period, but has not been used for this analysis; even so, the respectable resolution of the other tracking detectors, and the high statistics, result in a measurement of the lifetime that is the most precise to date.

2 The detector

The ALEPH detector is described in detail elsewhere [3]. A brief description of the features relevant to this analysis will be given here.

Close to the beam pipe is the inner tracking chamber (ITC), a cylindrical multiwire drift chamber with eight concentric layers of axial sense wires and a total of 960 hexagonal drift cells, with a maximum drift distance of 6 mm. The wire load is taken by the outer carbon-fibre wall, allowing the inner wall to be made of polystyrene to minimize multiple scattering, with a contribution of only 0.2 % of a radiation length to the thickness of material between the interaction point and the ITC wires (2.3 % in total).

Surrounding the ITC is a large time projection chamber (TPC), a cylindrical 3D imaging drift chamber of outer radius 1.8 m, with an axial electric field that is defined by a central membrane held at a potential of -27 kV. Electrons from ionization drift to the end plates, where they are detected by wire chambers with segmented cathode planes that provide measurements of up to 21 space points for charged particles traversing the full radius (for which the polar angle θ satisfies $|\cos\theta| < 0.79$). Charged particles within $|\cos\theta| < 0.96$ cross all eight layers of the ITC and at least four cathode pad rows of the TPC. Measurements of specific ionization ($\mathrm{d}E/\mathrm{d}x$) are provided by the TPC sense wires, with a resolution of 4.6% for 330 ionization samples, obtained for electrons in hadronic events.

Following detailed studies, the resolution of the tracking detectors is well understood [4]. The momentum resolution for tracks fit through both the ITC and the TPC is measured using dimuon events, $Z \to \mu^+\mu^-$, to be $\delta p/p^2 = 0.0008\,(\mathrm{GeV}/c)^{-1}$. The spatial resolution at the interaction point can be determined from the apparent separation of the two muon tracks at the origin, projected into the plane transverse to the beam axis (the $r\phi$ plane). From the *rms* width of this distribution, σ_S, a single track resolution of $\sigma_{track}(r\phi) = \sigma_S/\sqrt{2} = 140\,\mu\mathrm{m}$ is measured (for $p = 45.6\,\mathrm{GeV}/c$). This resolution is substantially better than that of about 1 mm along the beam axis.

The electromagnetic calorimeter (ECAL) is a highly segmented sandwich of wire chambers and lead plates, with a thickness of 22 radiation lengths, covering the angular region $|\cos\theta| < 0.98$. The position and energy of electromagnetic showers are measured using $3 \times 3\,\mathrm{cm}^2$ cathode pads connected to form projective towers, each read out in three separate stacks in depth corresponding to 4, 9 and 9 radiation lengths. For electromagnetic showers the energy resolution is measured to be $\delta E/E = 0.18/\sqrt{E}$ (E in GeV).

The ITC, TPC and ECAL are enclosed in a superconducting solenoid providing an axial magnetic field of 1.5 T. The 120 cm thick iron return yoke of the magnet is instrumented with $1 \times 1\,\mathrm{cm}^2$ streamer tubes to form the hadron calorimeter (HCAL), covering the angular region $|\cos\theta| < 0.99$. The barrel section of the calorimeter has 23 layers of tubes, whilst the end caps have 15 layers where they overlap the barrel and elsewhere 22 layers. The digital readout from the streamer tubes is used to identify muon candidates by providing a projective view of their tracks. This is assisted by muon chambers that surround the HCAL, of which one double-layer was installed for the runs used in this analysis. They are also constructed of streamer tubes at a 1 cm pitch, with two coordinates read out for each layer from cathode strips parallel and perpendicular to the wires.

The triggers for hadronic Z decays are described in detail elsewhere [5]. They depend on the energy deposited in the ECAL or a correlation between a track in the ITC and signals in the corresponding sectors of the ECAL or the HCAL.

3 Event selection

The event selection requirements are intended to select semileptonic B decays. They follow quite closely those used for the analysis of heavy flavour production, discussed in detail in Reference [6]. Only the salient features are described here.

Firstly hadronic events are selected by requiring that at least five tracks from the interaction region are reconstructed in the TPC, with a total visible charged energy greater than 20 % of the centre-of-mass energy. This has an efficiency of 95 % and a background from $\tau^+\tau^-$ and two-photon events of 0.3 %, determined using Monte Carlo data. Next, electrons and muons are identified; the strategy for each will be considered in turn.

Electron identification is achieved using two independent measurements: the energy deposition in the ECAL and the $\mathrm{d}E/\mathrm{d}x$ in the TPC. For the ECAL, two selection variables are defined to measure the extent to which the energy deposited close to the extrapolated track conforms to that expected of an electron. The first compares the measured momentum to the energy deposited in the four towers closest to the extrapolated track; the second depends on the mean position of the longitudinal energy deposition, as determined using the segmentation of the ECAL readout into three stacks in depth. These variables are required to be within 3 standard deviations of the value expected for an electron. For the TPC, the measured $\mathrm{d}E/\mathrm{d}x$ of a track is defined as the 60 % truncated mean of the individual wire measurements, where at least 80 isolated wire hits are required. The $\mathrm{d}E/\mathrm{d}x$ is required to be within 2.5 standard deviations of the value expected for an electron.

A background to the prompt electron signal comes from photon conversions and π^0 decays; this is reduced by rejecting candidates if they form an invariant mass of less than $20\,\mathrm{MeV}/c^2$ when paired with any oppositely charged track that is consistent with coming from a common vertex (*i.e.* with a distance of closest approach less than 1 cm in space). A second background arises from hadron misidentification; this is measured from the data using the independence of the $\mathrm{d}E/\mathrm{d}x$ and ECAL electron selection techniques [6]. The efficiency of the ECAL electron identification is measured to be 80 ± 2 % using electrons from photon conversions at the chamber walls that separate the ITC and TPC. With the additional $\mathrm{d}E/\mathrm{d}x$ requirement, the efficiency drops to 60–70 %, depending on the p and p_T of the track.

Muon identification relies on the digital streamer chamber readout of the HCAL and muon chambers. The cuts are designed to select penetrating tracks: a cone three times the *rms* displacement due to multiple scattering is defined around each track extrapolated through the HCAL, and muon candidates are selected according to the number of fired planes within that cone. A plane is considered to have fired if between one and four adjacent streamer tubes give hits, and candidates are required to have at least nine fired planes, with at least four of the last ten and one of the last three planes fired. For the data taken in 1989 only the HCAL barrel is used as the HCAL end caps and muon chambers were not fully operational; they are, however, included for the 1990 data, with the muon chambers providing an extra 3D point. The angular region $0.64 < |\cos\theta| < 0.68$ (at the overlap between the barrel and endcaps of the HCAL) is excluded for this analysis, as the limited instrumentation in this region leads to a higher level of background.

Backgrounds to the prompt muon signal come from charged pion or kaon decays which give nonprompt muons that satisfy the selection requirements, and from hadron misidentification. This may take the form of sail-through, where a hadron crosses the whole calorimeter without interacting, or punch-through, where an interacting hadron produces

one or more secondaries that exit the calorimeter within the multiple scattering cone. Punch-through is reduced by cutting on the number of hits in excess of those expected for a muon, lying within 25 cm of the candidate track. The efficiency of the muon selection is measured to be 83 ± 3 %, determined using dimuon events with correction from the Monte Carlo simulation to account for the presence of hadrons.

Quality cuts are next applied to the tracks of the electron and muon candidates. The momentum is required to be greater than $5\,\mathrm{GeV}/c$, which helps reduce both multiple scattering and the background from nonprompt leptons. At least five ITC hits and ten TPC hits are required, and the distance of closest approach of the track to the interaction point must be less than 5 mm in the $r\phi$ plane, and less than 3 cm along the beam axis. Only well fitted tracks are retained by requiring that the χ^2 per degree of freedom of the track fit is less than 3. Finally tracks are rejected that are compatible with coming from the decay of a K^0 or Λ by rejecting those which form an invariant mass within $30\,\mathrm{MeV}/c^2$ of these particles, when paired with any oppositely charged track that is consistent with coming from a common vertex.

Jets are then defined using all charged tracks in the event with momentum greater than $200\,\mathrm{MeV}/c$, using the scaled-invariant-mass clustering algorithm [7]. The transverse momentum of the lepton is determined relative to the jet axis, after first subtracting the lepton's momentum vector from the jet. The large mass of the b quark leads to a higher p_T on average for leptons from B decays than for those from particles containing lighter quarks, so B candidates are selected with a cut on the lepton p_T. For a cut at $p_T > 2\,\mathrm{GeV}/c$ there remain 2973 lepton candidates: 1215 electrons and 1758 muons. The B purity is estimated on the basis of Monte Carlo simulation to be about 73 %.

4 Impact parameter measurement

The impact parameter of a track, δ, is its distance of closest approach to the production vertex. The measurement of the production vertex position using tracks on an event-by-event basis is difficult in B events since a large fraction of the tracks originate from secondary vertices, and those that remain have low average momentum and suffer from substantial multiple scattering. Instead the centroid of the beam spot—the area over which the e^+ and e^- beams interact—is used as an estimate of the production vertex, determined over the period of a LEP fill. Since both the track resolution is best and the beam spot is smallest in the $r\phi$ plane, the impact parameter is projected onto this plane.

To form a variable which is sensitive to the lifetime, the impact parameter is signed according to the topology of the event, as illustrated in Figure 1. The direction of the parent B hadron is estimated using the jet axis. If the apparent flight distance of the parent hadron—the distance from the beam spot centroid to the point at which the lepton track crosses the jet axis—is positive, then the impact parameter is signed positive, and *vice versa*. Negative values can result from the finite tracking resolution, and can also arise if the jet axis does not reproduce the parent hadron direction well.

The position of the beam spot is determined by studying the distance of closest approach of tracks to the *coordinate origin* in the $r\phi$ plane, d_0. This quantity is signed according to the sign of the angular momentum component of the track along the beam axis, and in the absence of track distortions should have a distribution centred on zero. A value for the mean of the distribution of $\overline{d_0} = 0.4 \pm 1.9\,\mu$m is found for the tracks used in the resolution studies described below, indicating that any residual track distortions are small. If the beam spot is not centred on the coordinate origin, $\overline{d_0}$ has a sinusoidal dependence on the azimuthal angle ϕ. This is extracted from a least-squares fit, using all tracks in a fill with $p > 2\,\mathrm{GeV}/c$ and $|\cos\theta| < 0.80$. From the parameters of the sinusoid, the position of the beam spot centroid can be calculated, with a precision of $\sigma_{beam} \sim 30\,\mu$m for a typical fill.

As the centroid of the beam spot is taken as the estimate of the production vertex, the size of the beam spot will contribute to the error on the impact parameter measurement. For the optics of the LEP machine, the beam spot is expected to be elliptical in shape, with the horizontal width much greater than the vertical, due to synchrotron effects; the predicted dimensions are $\sigma_H = 200\,\mu$m and $\sigma_V = 10\,\mu$m, respectively. These dimensions can be checked using the data, by studying the variation with ϕ of the width of the d_0 distribution measured for tracks in hadronic events. Horizontal tracks ($\phi \sim 0°$) will see only the vertical size of the beam spot, whilst vertical tracks ($\phi \sim 90°$) will see the larger horizontal size, and their d_0 distribution will therefore be broader. Subtracting in quadrature the tracking error from the width of the d_0 distribution gives a measure of the beam spot size, and a clear dependence on ϕ is seen, compatible with the expected dimensions. These values are therefore assumed in the analysis that follows, although as will be seen the result is relatively insensitive to the exact choice. The small size of the beam spot is another advantage of LEP over previous e^+e^- machines for lifetime measurements.

The error on the measured impact parameter, σ_δ, thus has contributions from the following sources: the tracking error σ_{track}, which is taken from the covariance matrix of the track fit; the uncertainty on the beam spot centroid σ_{beam}; the size of the beam spot, with horizontal and vertical components σ_H and σ_V; and finally a contribution from multiple scattering in the material between the beam axis and the first measured point of the track in the ITC. The knowledge of the distribution of this material has been checked by studying the number of reconstructed photon conversions as a function of their materialization radius, which is found to be in good agreement with expectations. Using this knowledge of the distribution of material, the contribution from multiple scattering is calculated and is found to be small: $\overline{\sigma}_{MS} \sim 30\,\mu$m for tracks with momentum greater than $5\,\mathrm{GeV}/c$. Thus:

$$\sigma_\delta^2 = \sigma_{track}^2 + \sigma_{MS}^2 + \sigma_{beam}^2 + \sigma_H^2 \sin^2\phi + \sigma_V^2 \cos^2\phi\,. \qquad (1)$$

After these sources of error on the measured impact parameter have been taken into account, any remaining uncertainty is corrected in an average sense using the resolution function described below.

The impact parameter distribution for the selected B candidates is shown in Figure 2.

It is clearly skewed to positive values, with a mean of $142 \pm 7\,\mu$m. The B lifetime is extracted from a fit to this distribution, described in the next section.

5 Extracting the lifetime

An unbinned maximum likelihood fit is made to the impact parameter distribution, with contributions to the fit for the background sources as well as for the B signal. Wherever possible the data are used to determine the various contributions, in particular for the experimental resolution, although since the B decays are not fully reconstructed it is necessary to determine the underlying impact parameter distribution using Monte Carlo data. The Monte Carlo events were generated with a simulation of initial and final state radiation in the reaction $e^+e^- \to Z \to q\overline{q}$ [8], using the Lund model to simulate the parton cascade and hadron production [9]. The fragmentation of b and c quarks is described by the parameterization of Peterson *et al.* [10], and an updated decay scheme is used for charm and B mesons [6]. The Monte Carlo includes a detailed simulation of the ALEPH detector. For most of the studies mentioned here, a sample of 220,000 simulated hadronic decays was used.

The lifetime analysis follows quite closely that of Reference [11]. Five sources of the lepton candidates are considered:

1. Direct B decay;
2. Cascade B decay (via charm);
3. Direct charm decay;
4. Misidentification background: where a hadron has mimicked a lepton, as described in Section 3.
5. Decay background: true leptons but nonprompt, *i.e.* decays in flight and photon conversions.

The probability f_x that a lepton candidate comes from each of these sources (identified using subscripts $x = b,\ bc,\ c,\ mis$ and dec respectively) is determined as a function of the p and p_T of the track by a fit to the observed (p, p_T) spectrum, with the b and c fractions and fragmentation allowed to vary freely [6]; this analysis has been updated to take account of the running conditions over the full data-taking period. The p and p_T distributions are found to agree well between the Monte Carlo simulation and the data. The fitting function P for each event is then taken as the sum over the various sources of the probability that the lepton comes from a given source times a probability density function P_x which describes the expected distribution of impact parameters for that source:

$$P = \sum_x f_x P_x \,. \tag{2}$$

The probability density functions P_x will now each be considered in turn; their value will depend on the impact parameter and its error, and in the case of the prompt sources (b, bc, c) also on the lifetime of the parent hadron.

Firstly for the misidentification background, the distribution P_{mis} is determined using the data. Tracks are selected that satisfy all of the selection cuts used for the lepton candidates, *except* that they fail the lepton identification. The impact parameter distribution of these tracks is shown in Figure 3 (a). It has a positive bias since tracks from B and charm decays are included, and has tails from K^0s and Λs that have survived the cut intended for their rejection. The mean of the distribution is $33 \pm 3\,\mu$m, which agrees with the value of $36\,\mu$m found for Monte Carlo events. The tracks are then weighted with the probability f_{mis} that they would contribute to the misidentification background, and a fit is made to the impact parameter distribution, of a Gaussian plus exponential tails. The fit is used as a parameterization for P_{mis}.

The decay background distribution is expected to be broader than P_{mis}, since for example decays in flight give rise to kinked tracks that introduce an extra contribution to the impact parameter. This has been studied using Monte Carlo data: 15,000 events were generated with a single pion or kaon that is forced to decay before leaving the TPC, with a decay probability that is constant with distance. Their reconstructed tracks are required to satisfy the track quality cuts used for the lepton candidates, and the impact parameter of the muon from the decay is determined, signed with respect to the original hadron direction. Real hadronic events are then taken, and their tracks are replaced in turn with each of the simulated tracks that has corresponding generated momentum. The p_T of the original track, measured relative to the associated jet as for the lepton candidates, is scaled by the ratio of the reconstructed to generated momentum for the simulated track, and the track is kept only if it then satisfies $p > 5\,\mathrm{GeV}/c$ and $p_T > 2\,\mathrm{GeV}/c$. Next, the sign of the impact parameter must be determined: if the angle in the $r\phi$ plane between the jet axis and the hadron is smaller than the angle between the decay muon and the hadron, the impact parameter keeps its original sign; otherwise the sign will change for half the events on average, so both signs are kept with a weight of 0.5. The tracks are then weighted with their real decay probability, and with the probability f_{dec} that they would contribute to the decay background, and the resulting impact parameter distributions for kaons and pions are combined assuming a K/π ratio of $36 \pm 7\,\%$. The resulting distribution is shown in Figure 3 (b); a fit is made of a Gaussian plus exponential tails, which is used as the parameterization for P_{dec}. This procedure has been checked using the sample of 220,000 hadronic Monte Carlo events: the lepton candidates that pass all of the B selection cuts, and are identified (using the generator-level information) as coming from the decay background, have an impact parameter distribution that is found to be compatible with the P_{dec} parameterization. This sample also includes electrons from photon conversions, which, however, only account for 20 % of the decay background for the p and p_T cuts used.

For the prompt lepton sources, the contributions to the impact parameter distribution are separated into the convolution of an 'underlying' impact parameter distribution with

a resolution function, allowing the resolution to be determined from the data:

$$P_\ell = F_\ell(\delta, c\tau_\ell) \otimes R(\delta, \sigma_\delta) \ , \quad (\ell = b, bc, c) \ . \tag{3}$$

The underlying impact parameter distribution F_ℓ contains the dependence on the parent hadron lifetime τ_ℓ, and is determined from the Monte Carlo simulation. Events are selected that contain prompt leptons using the Monte Carlo generator-level information, and the lepton tracks are required to satisfy the selection cuts used for the real data. The true impact parameter of the lepton is determined relative to its production point (*i.e.* using the generated rather than reconstructed track), and to incorporate the possibility of sign errors it is signed using the *measured* jet axis. This distribution scales with the lifetime τ_ℓ, and can therefore be expressed as a function of $\delta/c\tau_\ell$, avoiding the need for Monte Carlo data generated with different input lifetimes. For the charm source an average value of 0.70 ± 0.20 ps is taken as the scaling lifetime, calculated bearing in mind the lifetimes, semileptonic branching ratios and expected relative production rates of the various charmed particles. For both the direct and cascade B sources the scaling lifetime is taken as τ_B, left as a variable parameter in the fit; for the cascade case this is justified since the initial B decay makes the dominant contribution to the impact parameter. A typical distribution is shown in Figure 3(c). A fit is made to the distributions using four exponential components, and is used as the parameterization for the underlying impact parameter distribution, in this case F_b. The distribution has a mean of 167 μm, whilst for F_{bc} the mean is slightly greater, 171 μm, and for F_c it is considerably smaller, 18 μm; in the absence of impact parameter sign errors (*i.e.* if the direction of the parent hadron was known exactly) the corresponding values would be 197 μm, 221 μm and 113 μm respectively.

Finally the resolution function $R(\delta, \sigma_\delta)$ must be determined. The error on the impact parameter σ_δ is calculated using the expression in Equation (1). The ratio δ/σ_δ for tracks from the interaction point should be normally distributed if the tracking errors are fully understood. To check if this is the case, tracks are used that satisfy all of the selection requirements for the lepton candidates, except lepton identification. These will still contain lifetime information, as was seen for the misidentification background; to avoid this, tracks are selected that have a p_T vector pointing substantially out of the $r\phi$ plane. Then their *projected* impact parameter should only be the result of resolution effects [11]. This is achieved by requiring that the polar angle of the track's p_T vector, θ_T, satisfies $|\sin\theta_T| < 0.5$. The resulting distribution is shown in Figure 3(d); the fit is of two Gaussians, which are well centred, indicating that lifetime information has indeed been reduced for the selected tracks. The central width is 1.07, close to ideal, but there are significant tails, at the level of 10 %, with width 2.6. These tails can come for example from the confusion of overlapping tracks, and they are taken into account by using the fit as a parameterization for R. The effect of bremsstrahlung on the electron tracks has been investigated, and following Monte Carlo studies the contribution of the tails to the resolution function is increased by 5 ± 3 % for electrons.

All of the parameterizations necessary for the lifetime fit have now been determined. Since those for F_ℓ and R are formed from Gaussian and exponential functions, their convolution can be calculated analytically. From Equations (2) and (3) the fitting function

for event i is given by:

$$\begin{aligned} P^i &= f_b F_b(\delta^i, c\tau_B) \otimes R(\delta^i, \sigma_\delta^i) + f_{bc} F_{bc}(\delta^i, c\tau_B) \otimes R(\delta^i, \sigma_\delta^i) + \\ & \quad f_c F_c(\delta^i) \otimes R(\delta^i, \sigma_\delta^i) + f_{mis} P_{mis}(\delta^i) + f_{dec} P_{dec}(\delta^i) \, . \end{aligned} \tag{4}$$

A likelihood function $\mathcal{L}$ is constructed as the product of the fitting functions for all events, $\mathcal{L} = \prod_i P^i$, and a fit is made by minimizing $-\log \mathcal{L}$. A single free parameter remains in the fit, τ_B, and the result is $\tau_B = 1.289\ ^{+0.058}_{-0.057}$ ps. The contributions to the fit from the different lepton sources are displayed in Figure 4; the fraction of the sample from each of the sources is 66 % from b, 7 % from bc, 10 % from c, 13 % from *mis* and 4 % from *dec*.

6 Checks and systematic errors

Several checks have been made of the measurement; the values obtained for the lifetime for different selection criteria are listed in Table 1. The analysis has been performed for the electron and muon candidates separately, and the lifetimes measured are found to be consistent. Similarly separation according to the sign of the lepton charge, or selection of tracks from a restricted region in the azimuthal angle ($|\sin\phi| < 0.5$, where the effect of the beam spot size is small), show no bias. The lifetime has also been measured for a sample selected with a lower cut on the p_T of the lepton track, $p_T > 1\,\mathrm{GeV}/c$, and the result agrees well with that for $p_T > 2\,\mathrm{GeV}/c$. Although the statistical error is smaller for the sample with the lower p_T cut, there is a larger systematic error due to the higher level of background.

As a further check of the method, the impact parameter distribution for tau leptons has been studied. The selection of $Z \to \tau^+\tau^-$ events is described elsewhere [12]; a sample of 4534 candidates are selected for the lifetime analysis, with 1:1 and 1:3 prong topology. The impact parameter distribution, measured with all tracks, has a mean of $44 \pm 3\,\mu$m. This agrees well with the expected value of $46\,\mu$m, determined using a Monte Carlo simulation with the tau lifetime set equal to the world average value.

Monte Carlo datasets have been generated with various input B lifetimes, from 0.0 ps to 2.6 ps, and have been passed through the full B lifetime analysis. In each case, the lifetime obtained is found to be compatible with that input, providing a check of the consistency of the procedure. For example, for the 220,000 hadronic events generated with an input lifetime of 1.3 ps, a value of $\tau_B(\mathrm{MC}) = 1.28 \pm 0.05$ ps is obtained.

Various possible systematic errors have been considered. The lepton source fractions f_x have some uncertainty; these uncertainties are determined from the fit to the inclusive lepton spectra, and are propagated through the lifetime analysis to evaluate their contribution to the systematic error by extending the lifetime fit to allow the source fractions to vary: $f_x = (1 + \epsilon_x) f_x^0$, where ϵ_x describes the extent to which the fraction changes from its nominal value f_x^0. This variation is constrained according to the errors on f_x by adding a quadratic term to the negative log-likelihood function:

$$-\log \mathcal{L} \to -\log \mathcal{L} + \frac{1}{2} \sum_{x,y} \epsilon_x C_{xy} \epsilon_y \, , \tag{5}$$

where C_{xy} is the covariance matrix for the source fractions. Thus the single parameter fit is extended to six parameters: τ_B and the five fractions f_x. As a result the error on τ_B increases, and that increase, in quadrature, is taken as the contribution to the systematic error of the lepton source fraction uncertainties. This same technique is used to account for the uncertainty associated with the various parameterizations used in the lifetime fit: P_{mis}, P_{dec}, F_b, F_{bc}, F_c and R. The parameters of each of the functions is allowed to vary in the fit, within its errors, using the full covariance matrix to include the effect of correlations between the different parameters.

There is a further contribution to the systematic error from the uncertainty on the K/π ratio for the decay background. The errors on the assumed average charm lifetime, and the enhancement to the tails of the electron resolution function due to bremsstrahlung, also make contributions. The beam spot dimensions used were varied by $\pm 50\,\%$, but the result was found to be relatively insensitive to such changes, due to their compensation on average by the resolution function. To check the effect of errors on the beam spot position, the position used was changed by $50\,\mu$m and the change of the measured lifetime taken as a systematic error. Finally, the B fragmentation affects the lifetime in two ways: it affects the lepton source fractions, as has already been taken into account in the uncertainty on those fractions, and there is a small residual dependence of the impact parameter on the B momentum. This effect depends on the fragmentation parameter $\overline{x}_B = \overline{E}_B/E_{beam}$ (the ratio of the mean B hadron energy to the beam energy), and from a simple consideration of the decay kinematics one can estimate:

$$\frac{\Delta\delta}{\delta} \sim \left(\frac{p_T}{p_L}\right)^2 \frac{\Delta\overline{x}_B}{\overline{x}_B}\,, \tag{6}$$

where $\Delta\delta$ is the uncertainty on δ induced by an uncertainty on $\overline{x}_B$ of $\Delta\overline{x}_B$, and p_L is the longitudinal momentum. The value $\overline{x}_B = 0.67 \pm 0.04$ [6] is taken, and leads to only a small systematic error contribution (in contrast to previous measurements performed at lower energies, where the sensitivity to uncertainty in the fragmentation is greater).

The contributions to the systematic error are summarized in Table 2. They are combined in quadrature to give a total systematic error of 0.10 ps.

7 Conclusion

A measurement of the average B hadron lifetime has been performed using the data taken by the ALEPH experiment at LEP over the period 1989–1990. From a total of about 170,000 hadronic Z decays a sample of 2973 B candidates is isolated by selecting identified leptons with $p_T > 2\,\mathrm{GeV}/c$. The B lifetime is extracted from a maximum likelihood fit to the impact parameter distribution of the lepton tracks, giving a value:

$$\tau_B = 1.29 \pm 0.06 \pm 0.10\,\mathrm{ps}\,, \tag{7}$$

where the first error is statistical and the second systematic.

Acknowlegement

It is a pleasure to thank the LEP division for the excellent performance of the machine. We also wish to acknowledge the contribution made to ALEPH by the technical staff of CERN and the home institutes. Those of us not from member states thank CERN for its hospitality.

References

[1] Mark II Collab., G. Abrams *et al.*, Phys. Rev. Lett. **62** (1989) 1236;
TASSO Collab., W. Braunschweig *et al.*, Z. Phys. C **44** (1989) 1;
DELCO Collab., W. Atwood *et al.*, Phys. Rev. D **37** (1988) 41.

[2] CLEO Collab., A. Bean *et al.*, Phys. Rev. Lett. **58** (1987) 183;
Mark II Collab., G. Abrams *et al.*, Phys. Rev. Lett. **64** (1990) 1095.

[3] ALEPH Collab., D. Decamp *et al.*, Nucl. Instrum. Methods A **294** (1990) 121.

[4] W. Atwood *et al.*, 'Performance of the ALEPH Time Projection Chamber', submitted to Nucl. Intrum. Methods A.

[5] ALEPH Collab., D. Decamp *et al.*, Phys. Lett. B **231** (1989) 519.

[6] ALEPH Collab., D. Decamp *et al.*, Phys. Lett. B **244** (1990) 551.

[7] W. Bartel *et al.*, Z. Phys. C **33** (1986) 23;
S.Bethke *et al.*, Phys. Lett. B **213** (1988) 235.
A value of 0.02 is used for the parameter y_{cut} of the algorithm.

[8] The DYMU program, J. Campagne and R. Zitoun, Z. Phys. C **43** (1989) 469.

[9] The JETSET 6.3 (Parton Shower) program, T. Sjöstrand and M. Bengtsson, Comput. Phys. Commun. **43** (1987) 367.

[10] C. Peterson *et al.*, Phys. Rev. D **27** (1983) 105.

[11] R. Ong, Ph.D Thesis, Stanford University, report SLAC-320 (1989).

[12] ALEPH Collab., D. Decamp *et al.*, Z. Phys. C **48** (1990) 365.

Selection	N_{event}	τ_B [ps]
Standard	2973	1.29 ± 0.06
Electrons	1215	1.27 ± 0.09
Muons	1758	1.30 ± 0.07
Positive charge	1515	1.22 ± 0.08
Negative charge	1458	1.35 ± 0.08
$\lvert \sin\phi \rvert < 0.5$	1045	1.34 ± 0.09
$p_T > 1\,\text{GeV}/c$	6218	1.27 ± 0.04

Table 1 Measurements of the B lifetime for different B candidate selections, as defined in the text.

Parameter	σ_{sys} [ps]
Lepton source fractions f_x	0.050
Misidentification background P_{mis}	0.010
Decay background P_{dec}	0.035
Underlying impact parameter F_b	0.050
Underlying impact parameter F_{bc}	0.010
Underlying impact parameter F_c	0.010
Resolution function R	0.040
Bremsstrahlung	0.030
Average charm lifetime	0.015
Beam spot size	0.005
Beam spot position	0.015
B fragmentation	0.010
Total	0.100

Table 2 Contributions to the systematic error.

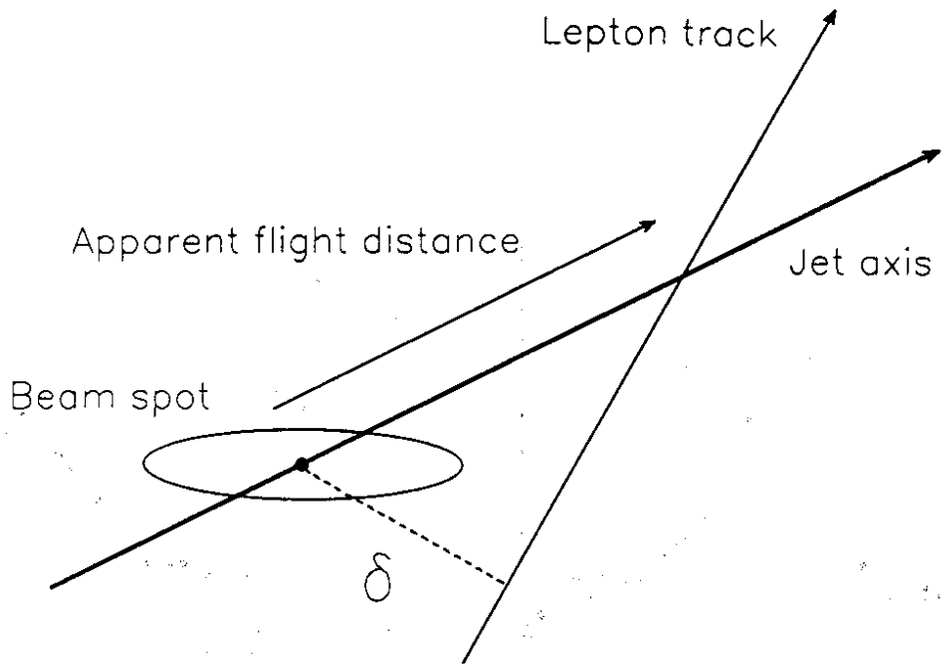

Figure 1 Definition of the impact parameter δ, in the plane transverse to the beam axis.

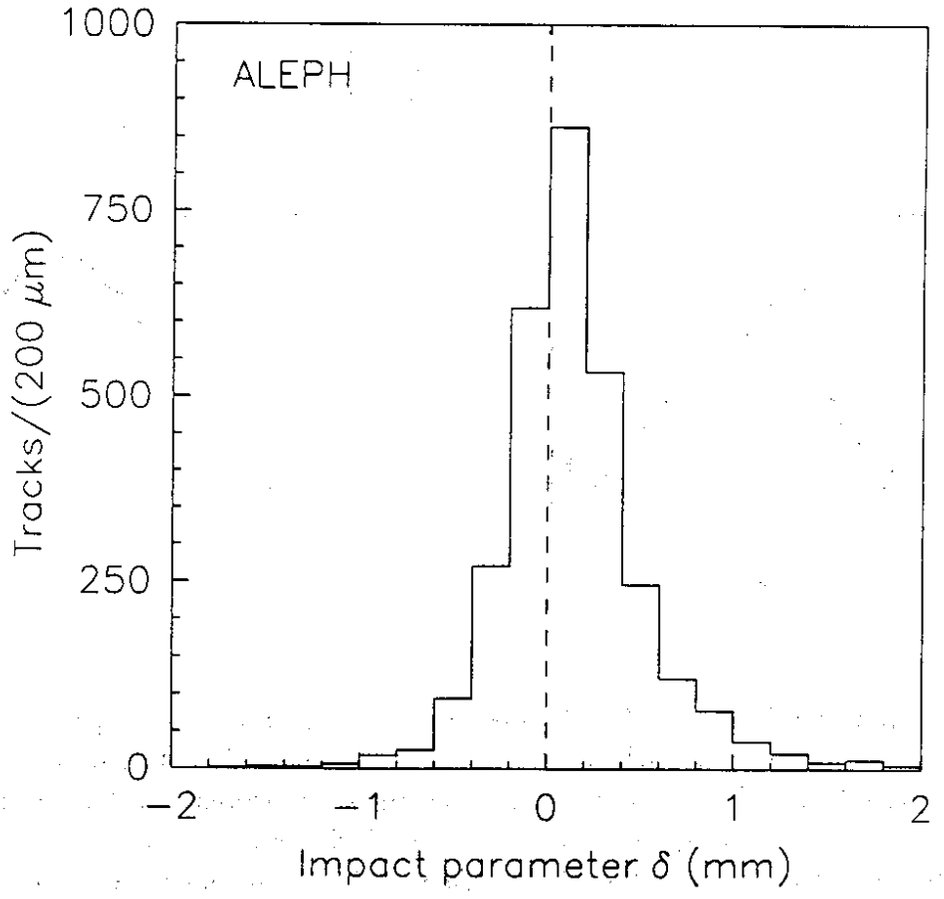

Figure 2 Impact parameter of lepton tracks that pass the B selection requirements.

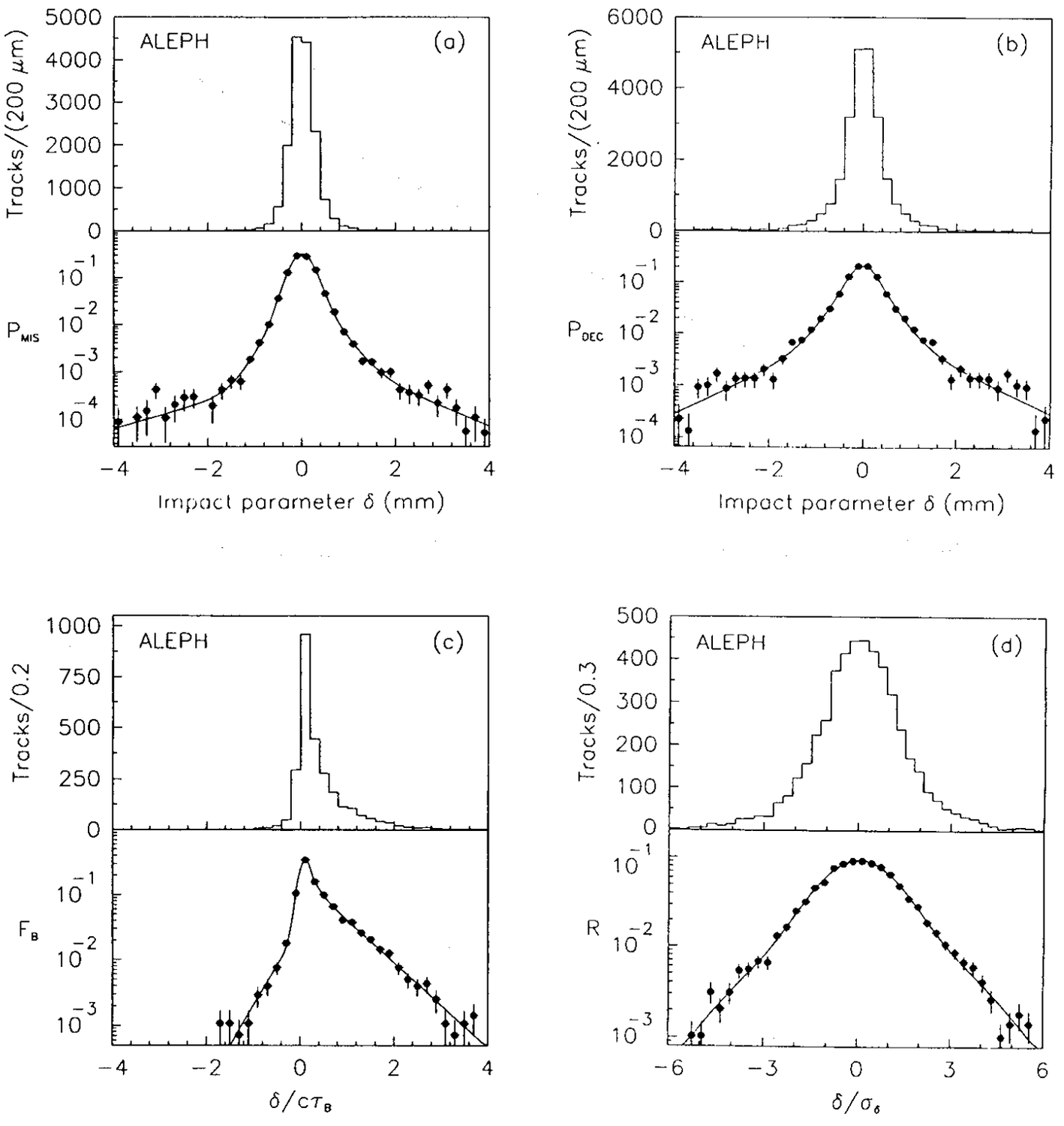

Figure 3 Parameterizations used for the lifetime fit. In each case the upper distribution is of tracks, with a linear scale, whilst the lower is normalized to the number of tracks with a superimposed fit and logarithmic scale. (a) Impact parameter of hadron tracks; (b) impact parameter of decay background tracks; (c) underlying impact parameter of leptons from B decays, determined using the Monte Carlo; (d) impact parameter divided by its error for tracks with p_T pointing out of the $r\phi$ plane.

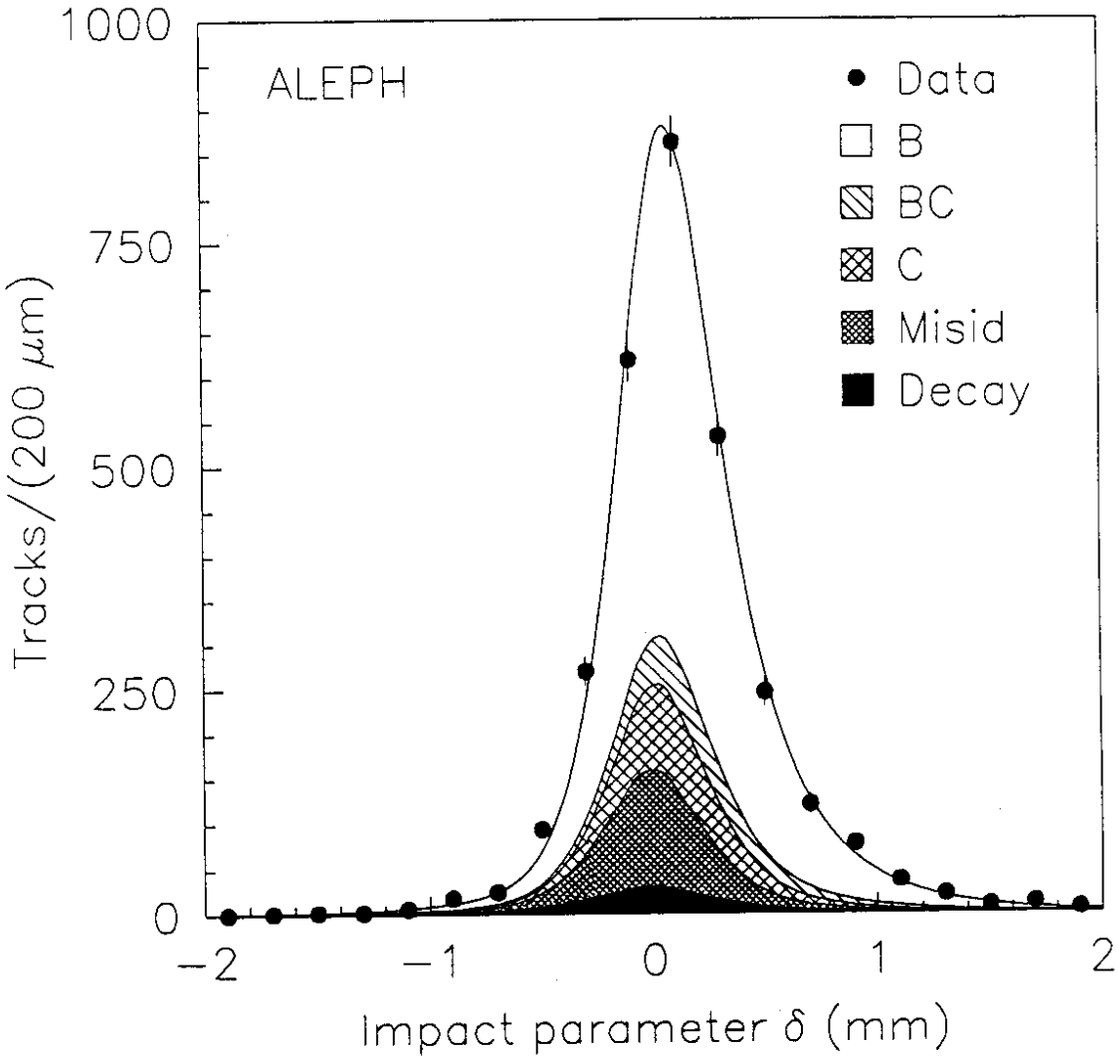

Figure 4 Impact parameter of lepton tracks that pass the B selection requirements, with the result of the lifetime fit superimposed. The contributions to the fit from the different lepton sources are shown.

Imprimé au CERN. Prix : 0.50 Fr.